FLITECAM – A near infrared camera for test and science applications on SOFIA

J. M. M. Horn[a], E. E. Becklin[a], O. Bendiksen, G. Brims[a], J. Goulter[a], E. Kress[a], N. Magnone[a], I. S. McLean[a], J. Milburn[a], N. Molayem[a], H. S. Moseley[b], M. Spencer[a]

[a]University of California, Los Angeles, Division of Astronomy and Astrophysics, 405 Hilgard Avenue, Los Angeles, CA 90095-1562

[b]Laboratory for Astronomy and Astrophysics, Goddard Space Flight Center, Greenbelt, MD 20771

ABSTRACT

As a facility class instrument on SOFIA, FLITECAM will be developed at the UCLA Infrared Imaging Detector Laboratory. Its primary purpose is to test the SOFIA telescope imaging quality from 1.0 to 5.5 microns, using a 1024×1024 InSb ALADDIN II array. Once the telescope test flights are finished, FLITECAM will be available to the science community. FLITECAM's field of view of $8'$ in diameter, with a plate scale of $0.47''$ per pixel, is one of the largest available for any facility camera. Grisms are available to provide moderate resolution of R≈1000-2000, depending on the slit width, with direct ruled ZnSe grisms. The detector readout electronics will be provided by Mauna Kea IR Inc. and is able to operate the detector array at all its planned operation modes, including occulations, telescope-nodding, high-speed shift-and-add, and optionally chopping at the longer wavelengths. Here we present our design approach to achieve those specifications. We also discuss the most important tests FLITECAM will carry out and give examples of science projects on SOFIA. For the latter, we present a preliminary list of filters which is expandable and open for discussions within the science community.

Keywords: SOFIA, Infrared, Instrumentation, Camera, Spectroscopy

1. INTRODUCTION

FLITECAM is the First-Light Infrared Test Experiment Camera on the Stratospheric Observatory For Infrared Astronomy (SOFIA). SOFIA, flying on a Boeing 747SP at altitudes of typically 41,000 ft, will operate above 99 % of the atmosphere's water content, leaving between 5 and 10 μm water vapor column above it.[1] Between 30 μm and 300 μm the atmosphere therefore becomes about 80 % transparent, with some atmospheric water absorption lines and almost spaceborne conditions between them. Between 4 μm and 600 μm are only relatively few atmospheric windows, which also depend on the water content, so that SOFIA has significant advantages there too. The telescope is being built in Germany and will be delivered to the SOFIA Science Mission and Operations Center in fall 2002. At that time, FLITECAM is intended to test the telescope performance.

FLITECAM is a near-infrared (1.0 - 5.5 μm) camera, using a 1024×1024 InSb ALADDIN array. The plate scale is $0.47''$ with an $8'$ circular field of view, which is identical to SOFIA's field. It is being built at UCLA as one of the facility instruments needed to support the joint assembly, integration, test and verification of the SOFIA telescope assembly during first light operations. FLITECAM will test the image quality, monitor the seeing, and establish the near-IR wavelength dependence of the seeing. After the test period, it will be available to the science community for general scientific use as a facility instrument. Scientifically, FLITECAM will provide wide-field imaging, narrow-band imaging and moderate resolution (R≈1300) spectroscopy, at wavelengths which are inaccessible from the ground. Also first light images for education and public outreach will be produced.

During the test phase, FLITECAM will often be jointly operating with the High-Speed Occulation Photometer and Imager (HOPI),[2] a special class science instrument on SOFIA, to run image quality tests simultaneously at visible and IR wavelengths. FLITECAM will also support occultation measurements together with HOPI, as well as independently. As FLITECAM will be testing the SOFIA telescope, its performance must be well established on

Further author information: (Send correspondence to J. M. M. Horn)
J. M. M. Horn: E-mail: horn@astro.ucla.edu, www: http://flitecam.astro.ucla.edu

other well-known telescopes before going on SOFIA. To accomplish this, the instrument will first be operated for several months at Lowell Observatory's 72-inch Perkins telescope in Flagstaff, AZ.

With 8′, FLITECAM will have one of the largest FOVs in the near-IR available to the science community. We are considering making use of FLITECAM's capabilities at the 3-meter Shane telescope at Lick Observatory on Mt. Hamilton, CA. FLITECAM operations at Lick, while other instruments are flying on SOFIA, are easy to establish due to the proximity of both observatories. Both the Perkins as well as Lick have f-numbers of f/17, which are close enough to the speed of the SOFIA telescope, which is f/19.6. Given that the f-numbers are relatively close, the nominal cold stop optimized for SOFIA, can be used for the Perkins and Lick telescopes as well without compromising the performance too much. For those ground-based applications as well as for calibration purposes, FLITECAM will not only have a filter set to specifically take advantage of the better atmospheric conditions, but also a standard ground-based filter set.

In the early stages, we planned to use a 1024×1024 InSb ALADDIN array on FLITECAM, re-imaging the entire SOFIA FOV at once. But due to problems at that time acquiring such big arrays, the design was descoped to use a single quadrant with 512×512 pixels, imaging only 4′ of the SOFIA FOV. The PDR review committee then strongly recommended the use of a full array, because the test program as well as the scientific program thereafter would benefit largely from such an upgrade. The investigation of the overall system performance with the larger field, and therefore with much larger optics, has shown satisfying results. We therefore implemented the review board's recommendation and present this new and larger design in this paper. One design goal, though, had to be omitted at least for first light, due to the upgrade. The originally planned high-resolution imaging mode will not be available on FLITECAM for first light. This mode, with a plate scale of 0.12″ per pixel, was part of the design in order to characterize seeing effects in the 1-5 micron range. Models based on KAO experience predict the best seeing between 3 - 8 microns. Going to shorter wavelengths, the seeing disk is expected to become larger, until the diffraction peak on top of the seeing disk disappears. With the high-resolution imaging mode, the diffraction peak on top of the seeing disk could be resolved. On the other hand, this mode will probably not be used that often once the test period is passed, and it was only a goal and not a strict requirement in the design with the smaller FOV. So in order to save space, complexity of the instrument and cost, we decided to not implement it for first light. A warm scale changer in front of FLITECAM might be available later to achieve higher spatial resolution.

FLITECAM is approaching the critical design review (CDR) in summer 2000. In an informal CDR on the optics design, the FLITECAM 8′ optics have been found to meet all its requirements. A detailed tolerance analysis has shown that all the lenses are manufacturable and that we are able to align them. The electronics system is well established by Mauna Kea IR Inc. and ordered.

First we will review the requirements on the FLITECAM design, which are mostly derived from the SOFIA test program. We then present the overall design before discussing the science applications

2. REQUIREMENTS

Most of the fundamental requirements imposed on FLITECAM are derived from the telescope test program and have been discussed earlier.[3] As the test program has evolved,[4] we will present the test requirements and their implications on the FLITECAM system design in more detail here.

2.1. Test-Plan Requirements

1. Telescope Focus
   In order to accurately and quickly focus the telescope, FLITECAM needs to have an automated focussing software tool. This is necessary to make other tests like assessing the image quality, etc. most efficient.

2. Image quality as a function of wavelength
   Special emphasis has to been placed on the performance between 3 and 5 microns, where the best seeing is expected, and where the advantages of conducting airborne rather than ground-based astronomy are biggest. So the plate scale of 0.47″ has been chosen to critically sample the best seeing at 5 microns which might be as good as 1.0″.

3. Telescope emissivity
   FLITECAM will have to measure the telescope emissivity, especially longward of 2.5 μm, in the L - and M - bands. This test has to be performed over the entire 8′ SOFIA FOV.

4. Monitoring the long-term background/seeing as a function of time
   The long-term seing will be measured as a function of wavelength, else the same considerations as under items 2 and 3 apply.

5. Telescope Pointing Stability
   A read-out speed of as fast as 100 μs per smallest sub-frame is required in order to freeze the shear layer and therefore to decouple image motion due to instability and image blur from optical performance.

6. Chopper performance
   The chopper performance will be tested for various chop frequencies and chop amplitudes. This test will be done simultaneously with HOPI, and it might not be available for first light on FLITECAM, as HOPI will have the ability to run those tests.

7. Dynamic IR background
   Here, the noise induced by changes in the amplitude of the background will be tested.

8. Water Vapor Monitor Calibration
   The water vapor monitor is a crucial instrument for SOFIA operations, as it will establish the contractually required measurement of the zenith water vapor overburden (WVO). Observations where the zenith WVO is above 10 μm do not count as successful flight hours. So at first light, this water vapor monitor needs to be calibrated. For this purpose, FLITECAM needs to have a spectroscopy mode with a resolution high enough to resolve unsaturated atmospheric water absorption lines in the 1-5 micron range. The line-of-sight water vapor needs to be measured with an accuracy of 1 micron. The resolution requirement also imposes a lower limit on the size of the pupil, as the diffraction limited resolution is proportional to the pupil size.

9. Characterization of the near-IR spectrum of the engine exhaust plume and scattered light from the engine tail cone
   At the lowest telescope elevations of about 20°, it is expected that scattered light from the engine tail cone will add to the background. Also, CO_2 emission lines from the exhaust plume will be detectable at those lower wavelengths.

2.2. Secondary Requirements and Constraints

1. FLITECAM has to provide an easy-to-use quicklook software tool in order to demonstrate IR astronomy, i. e. the generation of IR images, for education and public outreach.

2. On-time delivery to the SSMOC* and therefore early deployment at the Perkins telescope are essential to not delay the Observatory Operational Readiness Review, which is scheduled for December 2002. The test flights for FLITECAM and HOPI are from September to November 2002. Deployment to Perkins will be in fall 2001.

3. The entrance pupil has to be re-imaged in order to detect black spots on the telescope mirrors. E. g. small particles from the aircraft paint that come loose could fall onto the primary mirror, requiring cleaning. Also it could be established whether or not the mirrors need to be re-coated. The derived requirement for FLITECAM have been tightened. In order to critically sample a spot with unit emissivity, $\epsilon_s = 1$, on a clean mirror, $\epsilon_m = 0.04$, that increases the total emissivity of the primary by η=0.2 %, we need n_x pixels[3]:

$$\begin{aligned} n_x &= 2\sqrt{\frac{\epsilon_s}{\epsilon_m \eta}} \\ &= 224 \end{aligned}$$

   The constraints for the pupil viewing mode are therefore very loose, as we have four times more pixels available than needed.

4. The camera needs to pass FAA certification, and therefore has to be delivered with a full documentation package that includes complete drawings, stress analysis, and failure hazard analysis of all critical components.

5. The camera needs to be achromatic and not require re-focusing between wavelengths.

*SOFIA Science Mission and Operations Center

6. Sub-framing and fast readout are necessary in addition to chopping in order to not saturate the array at the higher wavelengths, L- and M-band, with the standard filter set.

7. Operations require frequent mounting and unmounting on SOFIA as well as on other observatories such as Lick and Perkins. Those procedures therefore have to be as easy as possible.

   Originally, it was planned that FLITECAM should have a Shack-Hartman test capability. This test would though be redundant, as HOPI will implement it too. Furthermore, it would complicate the FLITECAM optics design significantly, so that this mode has been dropped.

3. THE CAMERA DESIGN

3.1. Operations and System Design

As already mentioned, the camera will have three optical modes, low-resolution imaging, grism-spectroscopy and pupil viewing. A high resolution imaging mode will not be available for first light, but might be easy to achieve with a scale changer in front of FLITECAM later on. Operational modes are

- Stare
- Telescope Nodding
- Dither
- Chopping (might not be available for first light)
- Occultations.

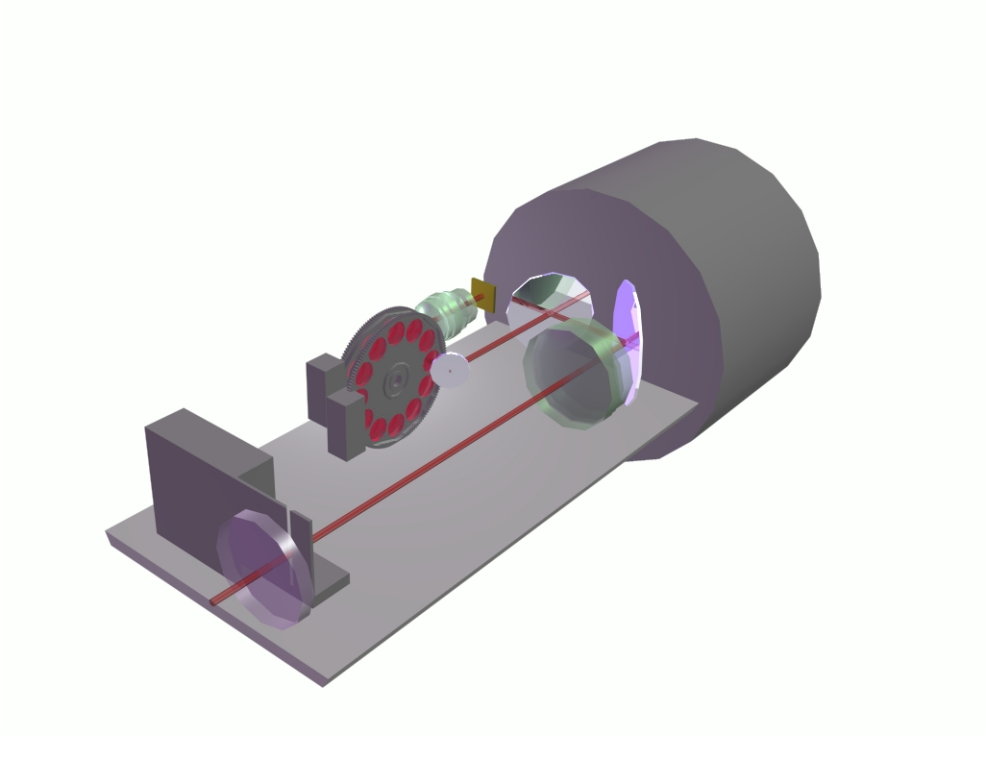

Figure 1. *The FLITECAM opto-mechanical layout. Shown is the window and aperture mechanism to the left, followed by the collimator, three fold mirrors and the double filterwheel with its two motors. Not visible is another fold mirror behind the filterwheels, which redirects the optical beam through the f/5 optics onto the detector. The Nitrogen can is located at the end of the cryostat. The outer diameter of the cryostat is 450 mm, and its length is 1.2 m.*

Detector	ALADDIN (InSb) 1024×1024 pixels
Read-Out Speed	$< 100\,\mu$s per smallest sub-frame (currently 16×8 pixels per quadrant) or $\gtrsim 12$ Hz full frame
Plate Scale	$0.47'' \times 0.47''$ per pixel
Field of View	$8'$ diameter
Wavelength range	1.0 - 5.5 μm for imaging L-band for pupil viewing
Spectral Resolution	R $\simeq$ 1300 with $2''$ slit
Camera Throughput	$\simeq 0.4$ in imaging mode $\gtrsim 0.38$ in pupil viewing mode
Point Source Sensitivity ($5\,\sigma$ - 1 h flux density, R=5, telescope emissivity=0.1, seeing: $2''$ in K, $1.5''$ in L,M)	K: 6 μJy, L: 20 μJy, M: 150 μJy
Smallest detectable black spot at primary	$\simeq 3$ mm

Table 1. *FLITECAM specfications summary*

Sub-framing will be possible in order to increase the read-out speed at higher wavelength, especially in the M-band, and not saturate the array. For characterization of seeing effects, the smallest sub-frames (about 16×8 pixels per quadrant of the array) can be read out in less than 100 μs. FLITECAM's InSb ALADDIN array is controlled by a read-out electronics system from Mauna Kea IR Inc. The specification of the camera are summarized in Tab. 1.

For normal operation, the detector needs to be cooled down to 30 - 35 K. Because there are no powerful closed cycle refrigerators available on SOFIA due to space and power restrictions, there are only a few other possibilities. One way to go would be to use a combination of liquid Nitrogen and liquid Helium. The use of liquid Helium though makes operations more complicated. We therefore investigated the use of a small Stirling cycle cooler which has been used already in astronomical instruments, cooling InSb arrays.[5] Those coolers have a limited cooling capacity, of the order of 1 Watt, which could be sufficient, if appropriately supplied to a well thermally shielded detector. We are looking into the possibility of using such a Stirling cycle cooler together with pumped nitrogen as coolants of our system. The pumped nitrogen would lower the radiation load onto the detector head and the limited cooling power of the Stirling cycle cooler would better be accomodated. This would also help to keep the thermal background from the optics even lower than with just LN_2. Tests are underway to determine the long-term temperature stability of the Stirling cycle cooler under load. The use of LHe rather than the Stirling cycle cooler is still a save fall-back solution.

The opto-mechanical layout is shown in Fig. 1. There are four mechanisms in the system, requiring one cryogenic operating motor each. An aperture mechanism will provide variable slit widths of $1''$ and wider and will open fully to provide an aperture stop. Furthermore, we need a double wheel for filters and grisms and a slide for pupil viewing lenses.

3.2. Optics

3.2.1. Imaging and Pupil Viewing

The FLITECAM optics design is considered frozen at this point. The performance optimization and tolerance analysis has been completed for the optics in both modes, f/5 imaging and pupil viewing, shown in Fig. 2. The optics, including imaging, pupil viewing, and grism spectroscopy, are described in detail elsewhere.[6] Here we present only the major performance results and specifications.

The basic performance requirements on the optics come from the SOFIA telescope design as listed in Sect. 2. The f/19.6 telescope produces an $8'$ circular FOV of 114 mm diameter. In order to re-image this FOV onto the detector with a plate scale of $0.47''$ per pixel, and a pixel size of 27 μm, an f/4.8 camera is needed. There has to be a collimated beam with a pupil image for placement of filters, cold stop, grisms, etc. The overall size of the optics is determined by the size of the pupil image and the FOV and shall be as small as possible in order to co-mount with HOPI. In order to still meet the performance requirements, there are limitations on getting as small a pupil as possible. We

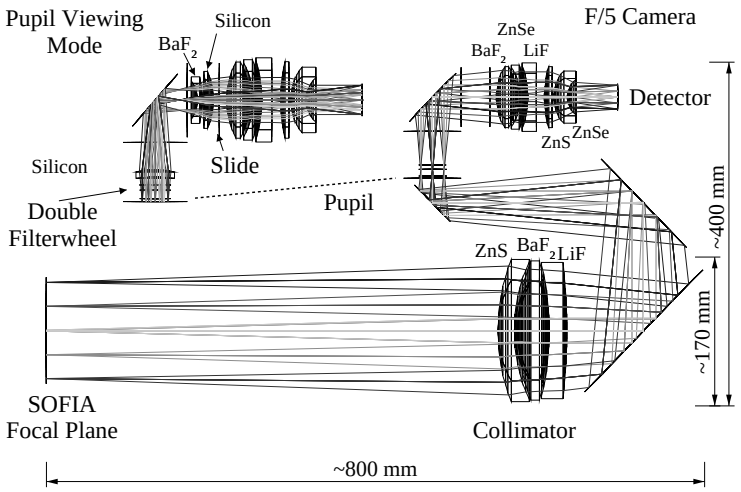

Figure 2. *The FLITECAM optics layout with the f/5 imaging mode being the default. The pupil viewing lenses are brought into the optical beam by means of a filter wheel and a slide. The pupil viewing mode from behind the pupil is shown in the upper left corner.*

found an f/5 collimator producing a pupil of 28 mm diameter to be about the fastest feasible. Although designed to be as compact as possible, the f/5 collimator triplet still has respectable lens diameters of about 170 mm and a total weight of 5.6 kg. A glass combination of ZnS-BaF_2-LiF has been found to fulfill the requirements for the following back-end camera and the pupil viewing mode. All lenses have spherical surfaces, and the SOFIA telescope has been included in the optimization process. The refractive indices used, were available from two independent sources.[7,8]

With this collimator we found a back-end camera that is achromatic over the entire wavelength range, having a wavefront error contribution of below 1/4 wave for all field angles and wavelengths, see Fig. 3. For the longer wavelengths though, the rms wavefront error is below 10 % for all field angles, which is reasonably close to the diffraction limit. The f/5 back-end camera is a split triplet consisting of BaF_2-ZnSe-LiF & ZnSe-ZnS. The last two lenses where necessary in order to compensate for spherical aberration. The diameter of the lenses varies from about

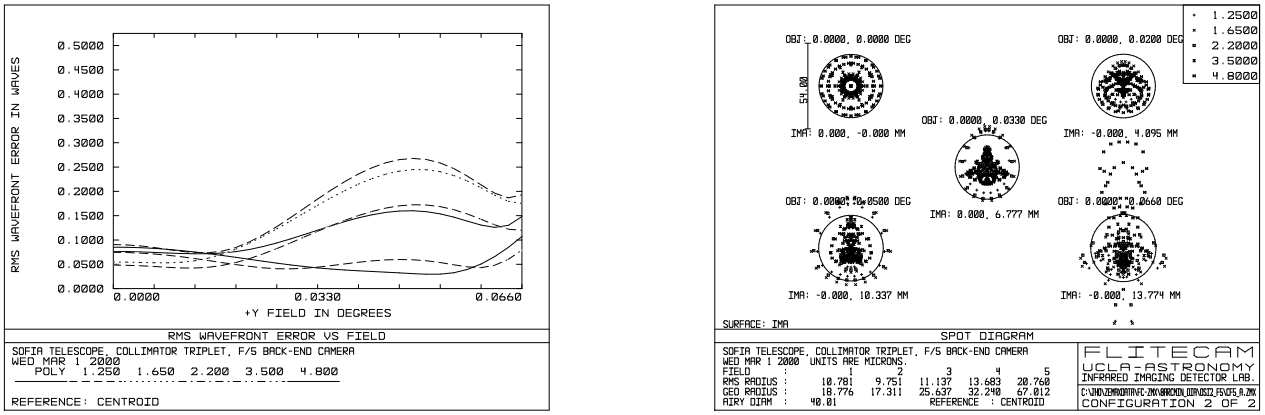

Figure 3. *RMS wavefront error and spot diagram for the imaging mode. The WFE diagram shows the approximate center standard band-wavelengths from the central field to the 8′ rim. The spot diagram is shows all wavelengths too, across the field of view.*

60 mm - 80 mm. The camera design, from the SOFIA focal plane on is shown in Fig. 2, see figure caption for more details.

The pupil viewing mode is achieved by inserting another set of 3 lenses between the pupil image formed by the collimator and the f/5 back-end camera. The pupil viewing triplet collimates the pupil rays which are then imaged onto the detector array by the f/5 camera, see Fig. 2. It consists of Silicon-BaF_2-Silicon, and is optimized for the short L-region, 3-3.5 microns. With diameters of 50 - 60 mm, those lenses are the smallest in the system, as they are close to the pupil. The performance of the pupil viewing mode has been found to be non-critical, and the major performance parameters, the wavefront error and the enpixeled energy diagram is shown in Fig. 4.

The design requires that there be space enough between the pupil and the f/5 back-end camera to insert filters, grisms, and the pupil viewing optics. Our design leaves sufficient space for a combination of a double filter wheel, carrying filters, grisms, and one of three pupil viewing lenses, and a slide mechanism carrying the other two pupil viewing lenses to accomodate all our different modes.

The window as well as the fluorides except LiF, will be coated, so that we get average transmissions for all lenses throughout the 1-5 micron range of about 95 %. The throughput is therefore about 40 % in the imaging mode, assuming a filter throughput of 80 % and taking the detector quantum efficiency of 80 % into account. The throughput in the pupil viewing mode will only be slightly worse, as an optimized, narrow-band coating can be applied.

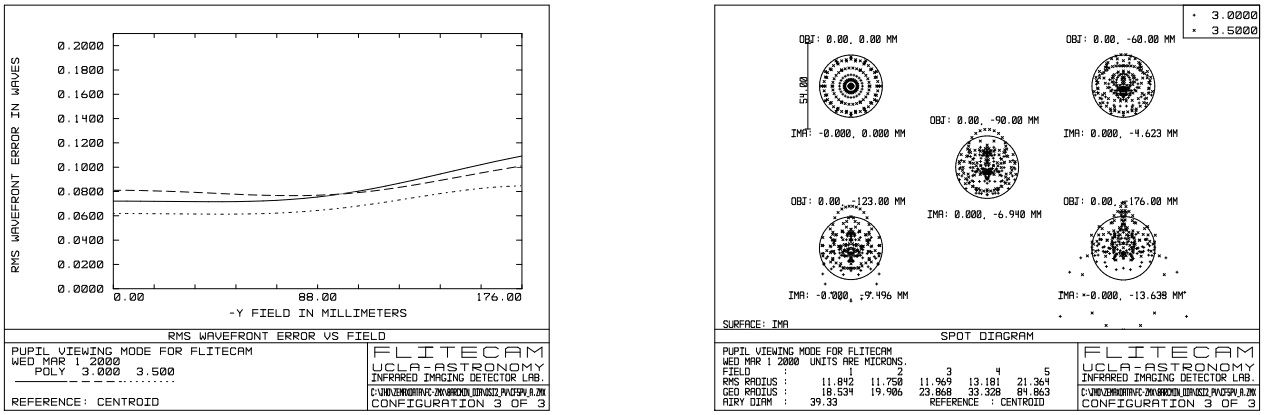

Figure 4. *RMS wavefront error and spot diagram for the pupil viewing mode. The WFE diagram shows the polychromatic performance throughout the field, reflecting the fact, that a 3.0 - 3.5 μm filter is used. The spot diagram is for 3.0 and 3.5 μm across the field of view.*

3.2.2. Grism Spectroscopy - Filter Selection

FLITECAM will have a variable slit width of about 1″ to >4″ in order to accomodate the expected worsening seeing from 5 μm to 1 μm. Assuming average conditions from 2.5 to 5.5 microns, the grisms for spectroscopy have been designed for a slit width of 2″.

In order to achieve a resolution of about R = 1300 for a slit width of 2″ and a collimator focal length of $f_{Coll} = 550$ mm, we are planning to use either ZnSe or KRS-5 (both n≃2.4) direct ruled grisms with an apex angle of 40°. The grisms have to be direct ruled, as resin grisms have an absorption feature at around 3.4 μm originating from an organic C-H stretch in the epoxy.

Under the conditions of Nyquist sampling of the smallest resolution elements and filling the entire array, the order-sorting filter bandwidths for two grisms, are plotted in Fig. 5. Each grism will be used in multiple orders (at maximum to fourth order), but not all possible order sorting filters will be implemented for first light. We will focus on the wavelength regions where no ground-based spectroscopy is possible. However, while comparing the standard filters with the grism orders, one can see that the standard J- and H-filters can be used for the 3rd and 4th orders

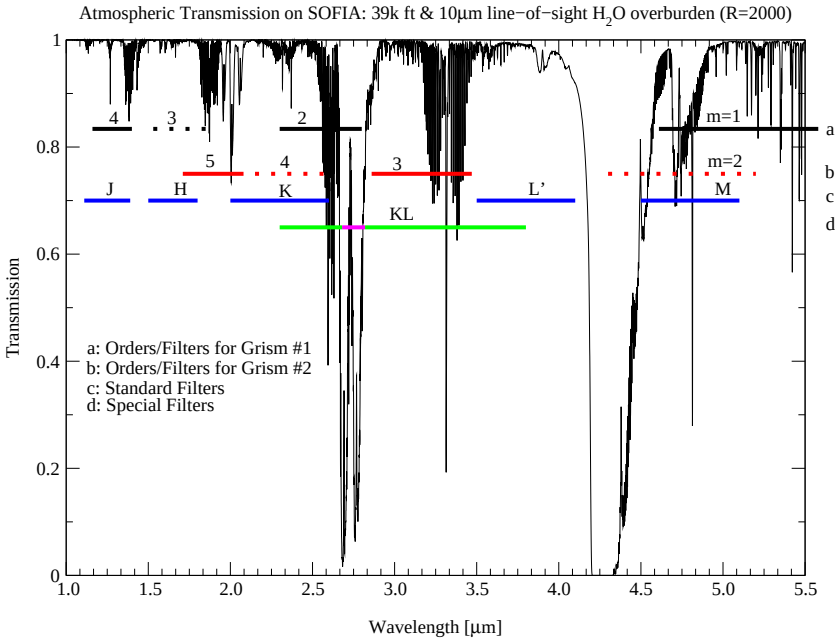

Figure 5. *Atmospheric transmission for a typical SOFIA altitude of 39,000 ft and a line-of-sight water vapor overburden of 10 μm for the FLITECAM wavelength range.*[9] *Overlaid are the spectroscopy filters, the standard filters and one special filter as planned so far. The dashed lines are grism orders where no filter is being planned. Note that the KL filter will have an obscuration at the atmospheric CO_2 lines. Not shown are narrow-band imaging filters.*

of grism # 1 and the M-filter falls entirely in the second order of grism # 2. Silicon immersion grisms,[10] as well as Germanium direct ruled grisms have been considered too. Those materials would yield even higher resolution due to their high refractive index (n(Si)≃3.4, n(Ge)≃4). However, the techniques of those grisms are currently still being developed, so that their implementation has been postponed. Special scientific projects could validate their acquisition during the first years of operation.

3.3. Mechanics

As any other instrument on SOFIA, FLITECAM needs to be FAA certified. So attention has been paid to mitigate risks where possible. Major parts, like the cryostat, will therefore be out-sourced to companies familiar with the FAA certification process, which is necessary for welding, for example. The less FAA critical, but scientifically crucial components like lens-mounts and mechanisms will be designed and fabricated in-house. Also where possible, existing designs like e. g. the double filterwheel and the slide will be used and upgraded where necessary.

The collimator mount however has to support large heavy lenses while placing them accurately enough to remain within tolerances. The mounts also have to be designed to flex to avoid thermal stresses at cryogenic temperatures. The present design is different from mounts previously used in near infrared instruments built at UCLA, NIRSPEC[11] and Gemini.[12] In the previous designs, the lens is held by flexible fingers aligned longitudinally (in the direction of the optical axis). The entire mount is fabricated from a single piece of aluminum.[13] The weight of the FLITECAM collimator, 5.6 kg, would flex those longitudinal fingers too much, so that the optical alignment tolerance on lens decenter, which is ±0.1 mm for each collimator lens, can not be met. The new design that we present here, orients the fingers along the circumference of the lens. A retaining flange on the back of the mount will guide the lens against a spacer to constrain it axially. Each individual spacer will rest upon a common reference plain in each assembly (see Fig. 6. The individual spacers help control each lens to maximum accuracy in order to hold it within tilt tolerances. This becomes critical on the first lens of the f/5 imager, where we will use the same lens mount concept. Finger flexibility can be estimated fairly accurately from its length, width and base dimensions. This proves crucial for a

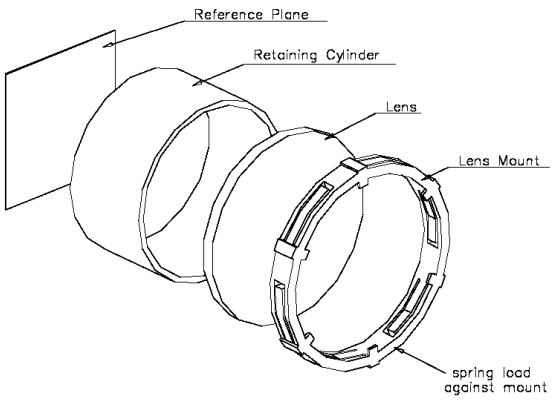

Figure 6. *The lens mount concept for the collimator triplet.*

few reasons. First, the weight of the collimator lenses may be enough to distort the mount under normal gravity (the heaviest lens in the assembly is approximately 2.4 kg). Second, since there is a fixed number of contact points, care must be taken to limit the pressure on the lenses. A finger pressing too hard could be damaging. The inner radius of the mount provides a maximum deflection point. From a worst case point of view, this radius must remain above the warm temperature diameter of the mounted lens at cryogenic temperature. This is the case if the lens mount cools extremely quickly, contracting around the lens. The mounts are still in the prototype stage. A dummy lens and test mount are to be made. Future tests will be run to help study the cold temperature reaction of the mounts and to refine their geometry.

3.4. Software

As a facility instrument on SOFIA FLITECAM will be available to the general science community. FLITECAM will also be mounted on at least one ground based observatory. The instrument software therefore needs to be user friendly and a simulation version of the software that is easily accessible to users in preparation for general investigator missions would be desirable. To achieve this goal, it is essential that the FLITECAM software be written in a platform independent fashion. However, the FLITECAM software must also interface with legacy code provided with the detector electronics from Mauna Kea IR (C++ and assembler) and take advantage of existing data reduction routines written in IDL,[14] e. g. These considerations constrain the basic software architecture of the FLITECAM instrument control software.

The FLITECAM software will be designed in a modular fashion to allow components to be incorporated into other instrument software packages. The software architecture used for FLITECAM, is shown in Fig. 7. The platform independence been achieved by using the Java[15] programming language rigorously down to the lowest level. Prototype studies have shown that Java can be used to control all of the internal mechanisms within the FLITECAM instrument. Since code written in C++, Assembler, and IDL will be used in critical areas of the software architecture, a middle-ware[†] communication technology is necessary to link FLITECAM Java code with the legacy code-base. To evaluate the available technologies, proto-type mechanism control systems were constructed using CORBA[‡] and a combination of RMI[§] and JNI[¶].[16] Although both systems were found to be workable the CORBA architecture was found to be easier to implement and inherently more powerful.

The core of the FLITECAM software design is the notion that each mechanical and electrical subsystem (filter wheels, slide mechanisms, temperature monitors) can be represented as distinct objects with specific properties. The FLITECAM software will control all of the mechanical and electrical assemblies of the instrument by manipulation

[†]'middle-ware' is a software communication protocol that allows code written in different computer languages to communicate with one another across a network

[‡]Common Object Request Broker Architecture

[§]Remote Method Invocation

[¶]JAVA Native Interface

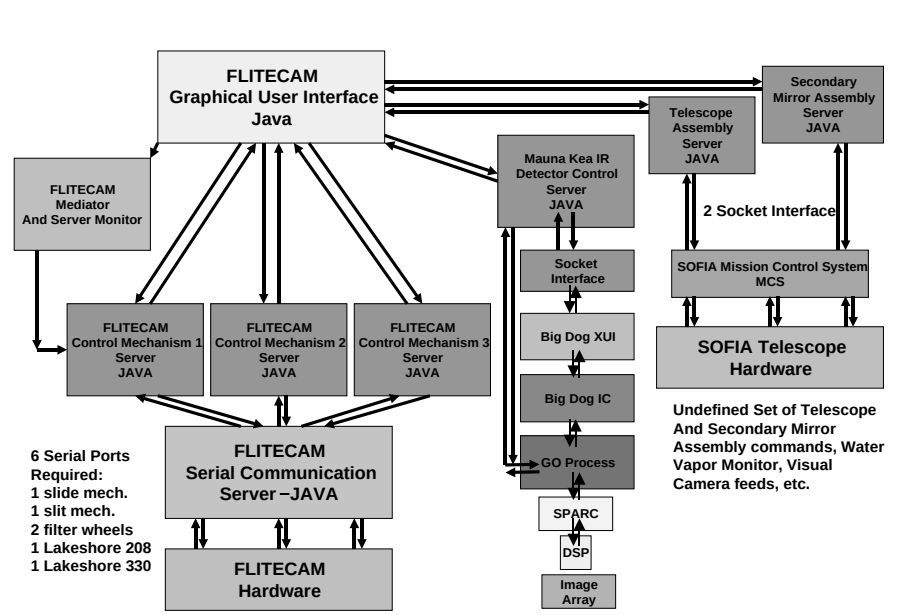

Figure 7. *The FLITECAM software architecture showing the key blocks and communication flow.*

of these objects. An abstract representation of the instrument and observatory components will be constructed in both the clients and the servers. The objects in the Java client will possess methods for changing the state of the instrument's subsystems. Since we want to be able to control multiple objects at the same time, each instrument object will run as a separate thread within the client and will be serviced by a separate server. By running in multiple threads it will be possible to simultaneously move two components at the same time without waiting for one operation to be completed. The instrument object model in the Java clients will be implemented as reusable Java Beans containing the core CORBA functionality. A preliminary version of the FLITECAM temperature monitoring and temperature control software has already been completed using this model.

The system will be a client / server implementation with multiple servers dedicated to control of individual mechanical and electrical subsystems. A mediator program will start and continuously monitor the multiple servers. CORBA will be used as the primary communication mechanism between clients and servers. Inprise's Visibroker 4[17] will be used as the preferred object request broker. Communication with legacy code provided by Mauna Kea IR will be handled by providing a CORBA interface to the C++ and Assembler code controlling the detector electronics. Image display and data reduction will use the extensive existing IDL code base by employing the ION server, which provides a Java interface to IDL. The resulting software system will have a completely platform independent client and a server architecture that can operate as a simulator on any platform. The software system will be deployed on a Solaris Sun 60S workstation connected to a SPARC station controlling the detector electronics. The system will allow FLITECAM to be remotely controlled from anywhere on a wide area network.

4. SCIENCE APPLICATIONS

Scientifically, the larger array and therefore larger field of view has important advantages over smaller ones. For example to survey the stellar population embedded in starforming regions would typically require observing fields of tens of arcminutes (e. g. Orion or M 16). Extragalactic studies of the starformation in spiral arms of nearby galaxies also requires large field of view. Number counts of galaxies that could be done at KL or at M, are more efficient with the $8'$ field of the full 1024×1024 array. Another interesting study would be deep integrations in KL, L or M in the Hubble deep field.

How efficient deep integrations in the near infrared are on SOFIA is shown in Fig. 8, where the background photon counts have been calculated[18] for two cases. In J, H, and K, the OH airglow[19,20] affects both airborne and ground-based observatories, as it is located above SOFIA's flight altitudes. The atmospheric absorption has been calculated

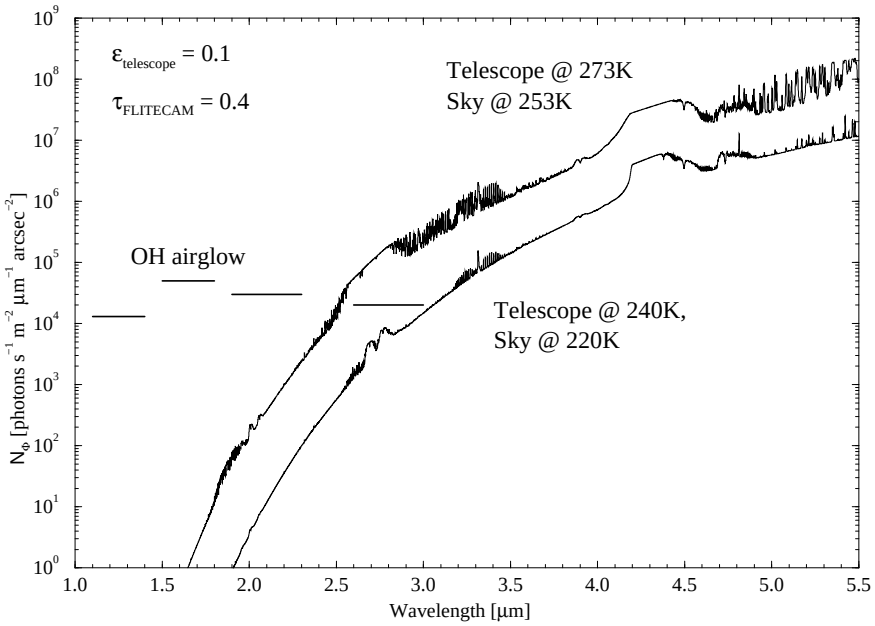

Figure 8. *The number of background photons per second per square meter of telescope aperture per micron wavelength interval and per square arcsecond, for a ground-based telescope (top curve) and for SOFIA.*

with 10 μm precipitable water along the line-of-sight for SOFIA, and 1 mm for the ground-based observatory. That figure shows that the 30 K difference between ground-based and airborne observatories has a significant impact on the background. However, to compile point source sensitivities and compare this with other large 8- to 10-m class telescopes, one has to take into account that their area compensates this advantage. Furthermore, the $\sim$0.5$''$ seeing of a good ground-based site has a strong impact on the point source sensitivity too. On SOFIA, the seeing is expected to be around 2.5$''$ in J and H, 2$''$ in K and around 1.5$''$ in L and M. The 5-σ 1-h flux densities for SOFIA translate[21] into J = 20.8 mag, H = 21.3 mag, K = 20.0 mag, L = 17.7 mag, KL = 19.0 mag, and M = 15.0 mag.

Another very important feature for FLITECAM is its ability to have moderate resolution grism spectroscopy of R$\simeq$1300. At such resolutions, spectra of brown dwarfs could reveal water and methane features, for example, which are difficult to detect from the ground.[22] And the richness of spectra in general longward of 2.5 microns has been shown by ISO.[23,24] The grisms have been designed to cover the most interesting regions, those which cannot be done at all or only rarely from ground (see Fig. 5). Some atomic and molecular lines which fall into the FLITECAM grism bands are Pa-α at 1.88 μm, Br-β at 2.63 μm,[18] and a C_2H_2 band at 2.6 μm.[23] A filter for the observation of PAH features at 3.3 μm[25] will be available too. The study of active galactic nuclei with spectroscopy of the Si VI line at 1.96 μm[26] could be efficient on SOFIA due to the good atmospheric conditions.

Narrow-band filters are not planned for first light, but will be available during the first year of operations. One possibility would be a set of Pa-α, and maybe Br-δ or Br-β. Independently, special filter sets can be implemented in the camera by guest investigator teams. That is true also for special grisms and filters if necessary. With high-index grisms made out of Silicon or Germanium, resolutions of R$\geq$2000 are possible.

ACKNOWLEDGMENTS

We would like to thank J. Larkin and J. Weiss for discussions on software and operations issues, J. Graham for the discussions test and science applications, E. W. Dunham for many helpful discussions during the project, and R. E. Fischer from Optics 1 Inc. for reviewing the optics design.

REFERENCES

1. E. F. Erickson, "SOFIA: The next generation airborne observatory," *Space Sci. Reviews* **74**, pp. 91–100, 1995.

2. E. W. Dunham and B. Taylor, "HOPI: high-speed occultation photometer and imager for SOFIA," in *Airborne Astronomical Systems*, *Proc. SPIE* **4014**, 2000.
3. D. F. Figer, I. S. McLean, and E. E. Becklin, "FLITECAM: a 1-5 μm camera for testing the performance of SOFIA," in *Infrared Astronomical Instrumentation*, A. Fowler, ed., *Proc. SPIE* **3354**, pp. 1179–1184, 1998.
4. E. W. Dunham and J. Horn, "The SOFIA Test Plan: 0.3 - 5.0 μm," Tech. Rep. TN-EWD-010.R2, NASA Ames Research Center, Moffett Field, CA 94035-1000, 2000.
5. T. P. OBrien and B. Atwood, "Indium antimonide detector cooling using a miniature split-stirling cycle cryocooler with coldfinger heat shunt," in *Infrared Astronomical Instrumentation*, A. Fowler, ed., *Proc. SPIE* **3354**, pp. 305–312, 1998.
6. J. M. M. Horn and I. S. McLean, "FLITECAM - a multipurpose near infrared camera for SOFIA," in *Optical and IR Telescope Instrumentation and Detectors*, *Proc. SPIE* **4008**, 2000.
7. J. T. Rayner, priv. comm., 1999.
8. H. Epps, priv. comm., 1999.
9. S. D. Lord, "A New Software Tool for Computing Earth's Atmospheric Transmission of Near- and Far-Infrared Radiation," NASA Technical Memorandum 103957, NASA Ames Research Center, Moffett Field, CA 94035-1000, 1992.
10. D. T. Jaffe, L. D. Keller, and O. Ershov, "Micromachined silicon diffraction gratings for infrared spectroscopy," in *Infrared Astronomical Instrumentation*, A. Fowler, ed., *Proc. SPIE* **3354**, pp. 201–212, 1998.
11. I. S. McLean, E. E. Becklin, O. Bendiksen, G. Brims, J. Canfield, D. F. Figer, J. R. Graham, J. Hare, F. Lacayanga, J. Larkin, S. B. Larson, N. Levenson, N. Magnone, H. Teplitz, and W. Wong, "The Design and Development of NIRSPEC: A near-infrared echelle spectrograph for the Keck II telescope," in *Infrared Astronomical Instrumentation*, A. Fowler, ed., *Proc. SPIE* **3354**.
12. I. S. McLean, B. Macintosh, T. Liu, L. S. Casement, D. Figer, F. Lacayanga, S. Larson, H. Teplitz, M. Silverstone, and E. Becklin, "Performance and results with a double-beam infrared camera," in *Infrared Instrumentation*, *Proc. SPIE* **2198**, pp. 457–466, SPIE, 1995.
13. L. S. Casement and I. S. McLean, "Optical design of an achromatic re-imaging lens system for a cryogenic near-infrared astronomical camera," in *Infrared Detectors and Instrumentation*, *Proc. SPIE* **1946**, pp. 569–580, 1993.
14. Research Systems Inc., 4990 Pearl East Circle, Boulder, CO 80301.
15. Sun Microsystems, 901 San Antonio Rd., Palo Alto, CA 94303.
16. Object Management Group, 250 First Ave., Needham, MA 02494.
17. Inprise Corp., 100 Enterprise Way, Scotts Valley, CA 95066.
18. A. T. Tokunaga, *Allen's Astrophysical Quantities*, ch. Infrared Astronomy. AIP Press, 2000.
19. M. J. McCaughrean, *The astronomical application of infrared array detectors*. PhD thesis, University of Edinburgh, Scotland, 1988.
20. F. C. Gillett, "Infrared arrays for ground-based astronomy," in *Infrared Astronomy with Arrays*, C. G. Wynn-Williams and E. E. Becklin, eds., 1987.
21. S. Beckwith, N. J. Evans II, E. E. Becklin, and G. Neugebauer, "Infrared observations of Monoceros R2," *ApJ* **208**, pp. 390–395, September 1976.
22. I. S. McLean, M. K. Wilkox, E. E. Becklin, D. F. Figer, A. M. Gilbert, J. R. Graham, J. E. Larkin, N. A. Levenson, H. I. Teplitz, and J. D. Kirkpatrick, "J-band infrared spectroscopy of a sample of brown dwarfs using NIRSPEC on KeckII," *ApJL* , April 2000.
23. J. Cernicharo, I. Yamamura, E. Gonzalez-Alfonso, T. de Jong, A. Heras, R. Escribano, and J. Ortigoso *ApJ* **526**, pp. L41–L44, 1999.
24. E. F. van Dishoeck, C. M. Wright, J. Cernicharo, E. Gonzales-Alfonso, T. de Graauw, F. P. Helmich, and B. Vandenbusche *ApJ* **502**, pp. L173–L176, 1998.
25. S. A. Sanford, Y. J. Pendleton, and L. J. Allamandola *ApJ* **440**, pp. 697–705, 1995.
26. A. Marconi, A. F. M. Moorwood, M. Salvati, and E. Oliva, "A [Si VI] (1.962 μm) coronal line survey of galactic nuclei," *A & A* **291**, pp. 18–28, 1994.